Journal of Applied Polymer Science

Polymer crystallization rate challenges: The art of chemistry and processing

Saša Andjelić, Robert C. Scogna
ETHICON, A Johnson & Johnson Company, ETHICON Surgical Care, R&D, Route 22 West Somerville, New Jersey 08876
Correspondence to: S. Andjelic (E-mail: sandjeli@its.jnj.com)

ABSTRACT: The intention of this study is to discuss scientific advances toward one very important challenge in the polymer processing industry: How does one increase the crystallization rate of slow-to-crystallize polymeric materials, thereby facilitating processing and enabling peak product performance? In the medical device field, where both government-controlled regulatory entities and medical professionals closely scrutinize the biocompatibility of added crystallization rate enhancers, achieving these twin goals has always been challenging. Herein, we present a review of various chemical and physical approaches used to tune the crystallization rate of semicrystalline polymers, with a strong emphasis on two novel approaches recently discovered and developed in our laboratories. © 2015 Wiley Periodicals, Inc. J. Appl. Polym. Sci. **2015**, *132*, 42066.

KEYWORDS: absorbable polymers; bimodal molecular weight; crystallization rate; hydrolysis; mixed initiators; polymer processing

Received 17 November 2014; accepted 9 February 2015
DOI: 10.1002/app.42066

BACKGROUND

The topic of polymer crystallization rates is a broad one, enveloping decades of research over a plethora of subdisciplines. For the purposes of this review paper, we focus on techniques, knowledge, and insights that allow the practicing polymer scientist to tailor the overall crystallization rate as required for success in downstream processing operations. For ease of discussion, we (somewhat artificially) sort these approaches into two broad groups:

1. Methods which require physical manipulation;
2. Methods which require chemical modification.

In so doing, we attempt to focus on the tools-of-the-trade most crucial for the working professional in the polymer science community, particularly those in the industrial sector. Of special interest to the authors are the absorbable polyesters so often used in the medical device community, and case studies from our own experience are presented for both of the aforementioned approaches.

The main focus of this review paper is the polymer crystallization rate. The overall crystallization rate is composed of two distinct parts: the nucleation rate and the crystalline growth rate. Nucleation represents the starting point for crystallization. Macromolecules arrange themselves in an organized pattern, forming a site onto which additional polymer chains will deposit, allowing the crystal to grow at a characteristic crystalline growth rate. Nucleation and crystalline growth rates are two independent components of the crystallization, and a variety of methods described below can be used to bias them one way or another. It is by the control of these two components that control over the overall crystallization rate may be achieved.

Methods Which Require Physical Manipulation

Strain or Flow Induced Crystallization. The application of strain to a polymer melt is known to increase crystallization kinetics.[1–3] This phenomenon is usually referred to as "Strain or Flow Induced Crystallization." The phenomenon is observed in many semicrystalline polymer systems, including polyethylene,[4–6] polypropylene,[6] other polyolefins,[4,6,7] polyethers,[8,9] and polyesters.[8,10] In the research laboratory setting, the applied shear profile is tightly controlled. Parallel plate,[11] rotational,[10,12] and channel flow[13,14] geometries are common. More complicated (albeit more industrially relevant) shear profiles, such as those experienced during injection molding[15] and melt spinning,[16] can also be examined using advanced synchrotron radiation techniques. Regardless of the deformation geometry used, substantial gains in the overall crystallization rate are realized when sufficient shear is provided, particularly when the extensional component of the deformation is large.[17,18] The time for crystallization may be reduced by up to several orders of magnitude, provided that the deformation rate is sufficiently high.[19]

In-depth investigations of strain induced crystallization (SIC) began with the pioneering rheo-optical work of R.S. Stein and

Saša Andjelić, Ph.D. is a Principal Engineer at Ethicon, a J&J company, working primarily in polymer R&D for implantable medical devices. With J&J for over 16 years, he has contributed to different areas including wound closure, adhesion prevention, hemostasis, drug delivery, antibacterial coating, as well as novel "green" chemistries for consumer products. Saša holds 21 US granted patents. He obtained his PhD degree in Polymer Science & Engineering at Polytechnic University, Brooklyn in 1998.

Robert Scogna, Ph.D. is a Senior Engineer with Ethicon, Inc., a Johnson & Johnson company. He successfully defended his doctoral thesis entitled "Morphological Origins of the Nonlinear Mechanical Properties of Semicrystalline Ionomers" at Princeton University in 2009. He currently works in the area of structure–property–processing relationships of semicrystalline, absorbable polyesters and their application in medical devices for wound closure, with the intent of continuous improvement of patient outcomes.

his collaborators in the 1960s and 1970s.[20–23] A direct correlation between the crystallization kinetics and applied strain/strain rate was observed. Since then, many studies have confirmed that extended polymer chains play an essential role in SIC. Kumaraswamy *et al.*[13] used *in situ* X-ray diffraction techniques to demonstrate that physical shearing creates long-lived, highly oriented structures often referred to as "shish."[24] Some researchers proposed that the high molecular weight fraction of a polymer forms the shish.[25] However, a recent small-angle neutron scattering study[26] concluded that the shish is not enriched in long polymer molecule concentration compared to the polymer on the whole. That being said, long molecules recruit other lower molecular weight material into the shish. Regardless of the mechanistic details surrounding shish development, the combination of applied strain and multimodal molecular weight distribution is an effective method for increasing the crystallization rate. Several studies[27,28] showed that the addition of a small quantity of ultrahigh molecular weight isotactic polypropylene (*i*-PP) to a matrix of lower molecular weight *i*-PP resulted in about a 10-fold increase in the crystallization kinetics when shear was applied to the polymer melt.

In cases where multiple crystalline phases can be formed, the application of shear can bias the relative abundance of each phase. Hsiao and coworkers discovered that in the case of *i*-PP, the competitive growth rates of the α and β phases may be tuned using shear.[11,29] The oriented α phase forms first and serves as nucleation centers for the β phase, which grow in afterward. By nucleating the β phase growth with the α phase, the overall crystallization rate is doubled.[11] The balance of nucleation and growth rates by the clever use of shear in conjunction with temperature control has been a useful technique, for example, in the medical device industry.[30]

Finally, the SIC phenomenon is not only found in polymeric melts but also in the solid state. For example, it is well known that chemically crosslinked rubbers often crystallize upon extension.[31] Extensional deformation requires neighboring polymer chain segments to align, thereby allowing them to crystallize. In this case, the crystallization is made favorable solely through the applied deformation and is easily reversed upon release of tension on the sample. That crystallization would occur upon extension has a clear thermodynamics basis; the increased amorphous phase orientation results in fewer possible conformations, thereby lowering the entropy (ΔS) and increasing the melting point (T_m) of crystals to a temperature greater than that of the sample ($T_m = \Delta H/\Delta S$). Pseudo-crosslinks formed by molecular entanglements[32,33] and end-group associations[32] may enable a small degree of SIC to occur, although elastomeric materials often experience permanent set upon extension and precise control of crystallization rate in these materials is generally not of significant commercial interest.

Physical Aging. The crystallization rate and degree of crystallinity of a polymer are strongly affected by its thermal history. Pan *et al.*[34] found that physically aging poly(L(−)-lactide) (PLLA), below its reported T_g of 60–65°C, at 40–50°C for 0–840 h significantly alters its crystallization rate. Aging increases the nucleation density and shortens the crystallization induction period. Fourier transform infrared spectroscopy results suggest that conformational rearrangements of the PLLA from the *gg* to *gt* conformer are likely responsible. The overall degree of crystallinity for some ethylene/α-olefin copolymers may slowly increase over the course of many months of room temperature storage[35] which is, of course, well over their T_g. This is due to gradual crystallization of short runs of crystallizable component, resulting in thin, secondary crystallites.[35–37] The slow growth of these secondary crystals can result in surprisingly large improvements in mechanical properties.[38–40]

Confined Crystallization. It is well known that the crystallization of low molecular weight species can be altered dramatically when confined to very small dimensions.[41] Similarly, macromolecular crystallization is strongly influenced by the geometry of the surroundings.

Ponting *et al.*[42] cast multilayer films of polycaprolactone (PCL) with either poly(methyl methacrylate) or poly(styrene). When the layer thickness is $\leq$75 nm, the film geometry templates the PCL crystallization resulting in large in-plane lamellae. Mass

transfer through the resulting films is reduced by up to two orders of magnitude.

The radial growth rate of semicrystalline polymer spherulites is generally linear with time.[43] However, polarized optical microscopy observations of PLLA films show that spherulitic growth rates are nonlinear prior to impingement when confined by geometrical constaints.[44] Others argue that nonlinear spherulitic growth rates can be explained by nonsteady state conditions that are experienced.[45]

On the other hand, crystallization in some ultrathin polymer films is severely impaired. Crystallization rates for ultrathin films of 3-hydroxybutyrate,[46] PLLA,[47] and poly(ethylene terephthalate)[48] (PET) were strongly depressed—and eventually completely arrested—as film thickness was reduced. Dielectric spectroscopy studies[47,48] have elucidated that the suppression of crystallization in ultrathin films is not solely due to size effects. There is strong evidence to support the notion that irreversible adsorption of chains at the film surface impairs local chain mobility (relative to the bulk) and hinders crystallization.

Finally, confined crystallization can alter semicrystalline polymer properties other than the crystallinity and crystalline architecture. For example, the glass transition temperature (T_g) of PLLA decreases by as much as 30°C when crystallized under partially constrained conditions.[49] At the same time, there is no marked effect on the melting point, heat of fusion, and overall degree of crystallinity for this polymer system.

Phase Separation. Crystallization behavior may be markedly impacted by the effects of phase separation. Jin and coworkers[50] found that blending *i*-PP with polyolefin block copolymers results in blends with far greater nucleation density than pure *i*-PP. The nucleation changes are ascribed to the large amount of interfacial area generated by the spinodal decomposition. Moreover, the nucleation density, isothermal crystallization rates, and linear growth rate were found to be compositionally dependent[51]. Pan *et al.*[52] found that blends of 10–25% poly(vinylidene fluoride) with PLLA resulted in a two to three order increase in the PLLA nucleation density, another example of enhanced crystallization in dual semicrystalline blends. Arai *et al.*[53] found that crystallization rates for liquid–liquid blends of poly(ethylene glycol) (PEG) and poly(methyl methacrylate) were substantially higher than observed in pure PEG systems, due to simultaneous phase separation and crystallization. Nanoscale phase separation in ordered block copolymers can also template crystallization, forcing the crystallization kinetics to adopt various kinetics depending upon the details of the microphase geometry.[54]

Bimodal Molecular Weight. The overall crystallization rate can be altered by judicious choice of molecular weight distribution. For example, adding a small to moderate amount of relatively high molecular weight material to a matrix of lower molecular weight is a potential strategy for altering the crystallization rate.[55,56] This approach works best for materials with impeded nucleation kinetics. The bottleneck to crystallization in other materials is not nucleation, but the crystal growth rate. Recently, blends of high and low molecular weight poly(ethylene oxide) were noted to exhibit counterintuitive behavior: the greater the content of low molecular weight material, the slower the spherulitic growth rate.[57] The resulting hypothesis was that increasing the number of chain ends results in more crystalline defects at the crystalline growth front.

Changing the molecular weight distribution can also impact the crystalline macrostructure. Elmoumni *et al.*[58] found that the macrostructure of blends of high and low molecular weight *i*-PP could be altered from spherulitic to shish-kebab through the application of mechanical shear. A critical Weissenberg (Wi) number—a function of both the blend ratio and total shearing time—describes the critical amount of shear needed to transform a material from one texture to another.

The use of multimodal molecular weight distributions as a technique for tuning semicrystalline polymer crystallization rates has been explored in our laboratories. As discussed in the Case Study 1 below, Andjelić and Fitz have found that the "Bimodal Molecular Weight" technique is a very promising new technology for semicrystalline polyesters used in the medical device industry.[55,56]

Methods Which Require Chemical Modification

The Addition of Nucleation Agents. The deliberate addition of foreign seed material to a polymer melt to encourage nucleation is a common strategy. This is particularly effective when the crystal growth rate under process conditions is favorable, but while homogeneous nucleation (i.e., the ability of a material to self-organize into a suitable nucleus) for the given polymer is unfavorable. Nucleating agents come in many varieties, including (but not limited to) organic salts,[59] organic acids,[60] carbon black,[60] talc,[61] layered metal phosphonates,[62] sodium hydroxide or bicarbonate,[60] carbon nanotubes,[63] and pigments.[60] Nucleating agents are generally added in very low amounts (often < 0.1 wt %) and can function either by promoting epitaxial growth or by inducing chemical reactions which promote the formation of a new nucleus.[59] The search for an effective nucleating agent for a given polymer system may be arduous and may require screening of hundreds,[64,65] or even thousands,[66] of compounds.

In the area of synthetic absorbable polymers typically used in medical applications, it has been described that a finely ground polyglycolide, with its high melting point, can serve as a nucleating agent for lower melting absorbable resins.[67] Small amounts of nucleation agents such as uracil and orotic acid are effective in significantly improving the crystallization properties of PLLA and poly[(3-hydroxybutyrate)-*co*-(3-hydroxyhexanoate)].[68–71] Outside of deliberate attempts to add nucleation agents, researchers have also discovered that low-level impurities, such as residual catalyst,[59] can impact the crystallization rate. Even reagents used in the polymerization process can play a role, in some cases indirectly increasing the polymer crystallization rate. Case study 2, presented below, will present one such experience.

Environmentally Induced Crystallization. The environment surrounding a polymer can strongly impact the crystallization rate. For example, López-Rubio *et al.*[72] showed that the combination of heat and humid surroundings allow an otherwise

Table I. Selected Properties of Dried 92/8 PDO/Gly Copolymers Made by a Single Initiator (Example 1), and by Mixed Initiators (Examples 2–3)

Copolymer ID	IV[a] (dL/g)	M_w[b] (g/mol)	MI[c] (g/10 min)	Polymerized PDO (mol %)	Polymerized Gly (mol %)	PDO monomer (mol %)	Glycolide monomer (mol %)
Example 1	1.75	65k	0.149	91.4	7.5	0.9	0.1
Example 2	1.63	60k	0.212	91.7	7.5	0.7	0.2
Example 3	1.95	74k	0.099	91.6	7.7	0.6	0.1

[a] IV was determined in hexafluoroisopropanol (HFIP) solution at 25°C at concentration of 0.1g/dL.
[b] Weight average molecular weight as determined by GPC.
[c] Melt index measurements (MT987 Extrusion Plastometer, Tinius Olsen, Willow Grove, PA) were conducted at 150°C using 6600 g disc. The die diameter was 0.066 cm, while the die length was 0.800 cm.

amorphous polyamide to crystallize, resulting in a noticeable increase in barrier properties with respect to oxygen as well as a reduction in water sorption. The hypothesis put forward is that the moisture disrupted amide group self-association, thereby plasticizing the amorphous chains and inducing sufficient mobility to promote crystallization. The T_g drops due to a loss of intrachain and interchain hydrogen bonding. In another example of environmentally induced crystallization, Porter and Yu[73] found that the isothermal crystallization kinetics and degree of crystallinity of poly(3-hydroxybutyrate) are a function of both temperature and pH.

Solvent Induced Crystallization. Polymer crystallization may be altered by surrounding the material in an environment containing organic solvents (a special case of environmentally induced crystallization). Polymers may be soaked in a liquid-phase solvent[74] or simply exposed to vapor enriched in the solvent(s) of choice.[75] In most cases, the uptake of solvents by polymer is non-Fickian[76] due to swelling and multiple polymer chain segmental relaxations. This approach has been successfully demonstrated in a number of polymeric systems, including PET,[74,75,77,78] and cellulosic polymers.[79,80] A special case of solvent induced crystallization is the use of supercritical CO_2 as a plasticizer to aid in crystallization rate. This approach has been used successfully in Bisphenol A polycarbonate[81] and poly(lactic acid).[82]

Reducing Molecular Mobility. Suppressing polymer chain mobility typically results in an increase in the T_g. Since crystallization kinetics are prohibitively slow near the glass transition, it is expected that this change would reduce crystallization kinetics, all other things being equal.[83] There are, however, exceptions. For instance, an introduction of amide linkages into PET and poly(-butylene terephthalate) increases the T_g, flexural moduli, and especially their crystallization rates.[84] The proposed mechanism of these polyester amide copolymers is self-association of amide groups through hydrogen bonding. Self-association reduces segmental motion; the vitrified amide-rich regions within the copolymer are thought to serve as nucleation sites for crystallization.

In the case of gamma-irradiated ultrahigh molecular weight polyethylene (UHMWPE), other interesting crystallization behavior was reported.[85] Network formation (*a.k.a.*, crosslinking) prevails over chain scission processes in *in vacuo* irradiated samples, consequently lowering the overall crystallinity level of the polymer due to imposed geometrical constrains. However, the presence of "melt-resistant," ordered grains discovered in irradiated UHMWPE samples causes a progressive chainlike nucleation that proceeded along the edges of these domains. In a separate effort, Dikovsky *et al.*[86] showed enhanced crystallization rates in melt blends of UHMWPE and *i*-PP (up to a 1 : 10 ratio), as monitored by *in situ* wide- and small-angle X-ray scattering (WAXS and SAXS, respectively). Shear flow aligns the fibrillar UHMWPE domains which, in turn, hinders the relaxation of *i*-PP chains and allows the aligned *i*-PP chains to create a shish-kebab microstructure.

The existence of a network structure can, in certain cases, lead to a very unique crystallization response.[87] In the late 1980s, Loomis and Murdock discovered a stereocomplex formation in absorbable polylactide systems.[88,89] Blending of roughly equimolar quantities of poly(L(−)-lactide) homopolymer and poly(D(+)-lactide) homopolymer results in the formation of poly(L(−)-lactide)/poly(D(+)-lactide) stereocomplexes. These systems exhibit higher T_gs, melting points, degree of crystallinity, and faster crystallization rates as compared with either of the individual blend components. By leveraging the higher melting point of the stereocomplex, self-nucleation of polylactide was explored by blending small amounts of poly(D(+)-lactide) homopolymer into poly(L(−)-lactide) homopolymer.[90] It was found that small crystals of the stereocomplex formed and acted as nucleation sites to speed up crystallization.

EXPERIMENTAL

The experimental details of the procedures used in the Case 1 studies presented herein can be found elsewhere.[55,56,91–93] Additional experimental data used in conducting the Case 2 studies are given below. Standard error for all data types is estimated to be <5% for all analyses used, unless otherwise stated.

Synthesis of Block Poly(*p*-dioxanone-*co*-glycolide) Copolymers

A block copolymer, *p*-dioxanone-*co*-glycolide (PDO/Gly), was prepared by ring-opening polymerization using mixed initiators in a metal reactor outfitted with a suitable agitator, as described below, using stannous octoate (Air Products and Chemicals, Allentown, PA); total Tin 29% w/w at a monomer-to-catalyst mole ratio of 30,000 : 1, using a 50 : 50 mole ratio of monofunctional initiator, dodecanol (DD, Fisher Scientific, Fairlawn, NJ), to a difunctional initiator, diethylene glycol (DEG, Fluka Chemie AG, Buchs, Switzerland). As a control, we also synthesized the copolymer with a single initiator (DEG).

The preparation of the PDO/Gly copolymers is a two-stage block copolymerization. The first stage homopolymerization

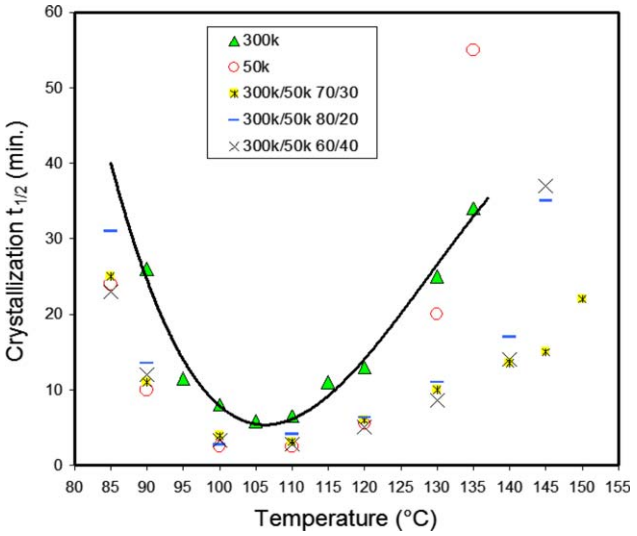

Figure 1. Isothermal crystallization kinetics of two PLLA homopolymers (M_w = 300k and 50k) and their respective bimodal molecular weight blends as measured by DSC. The figure is reprinted from the patent literature.[51,52] [Color figure can be viewed in the online issue, which is available at wileyonlinelibrary.com.]

was conducted using 100% *p*-dioxanone, and a second stage block copolymerization was done with an added monomer composition of 100 mol % glycolide. After the second stage, unreacted *p*-dioxanone and glycolide monomers were removed by vacuum drying procedure. The overall final composition of dried samples, as determined by ^{1}H NMR analysis, revealed a copolymer of about 92 mol % polymerized *p*-dioxanone and 8 mol % polymerized glycolide. To achieve this desired chemical composition, the initial monomer charge was higher in *p*-dioxanone monomer: 94 mol % PDO and 6 mol % glycolide.

Further details of the synthesis, drying, and grinding steps can be found elsewhere.[86] An example of resins prepared using a single initiator only (DEG) and combination of initiators (50 : 50 DD : DEG) is given in Table I.

Monofilament Extrusion of 92/8 Block PDO/Gly Copolymers

Extrusion runs on 92/8 block PDO/Gly copolymers were conducted using two monofilament extruders: one inch JJ Jenkins Extruder with 18 : 1 barrel length and one inch Davis-Standard Extruder with 24 : 1 barrel length equipped with a single grooved feed throat.

Both JJ Jenkins and Davis-Standard extrusion lines use a water bath tank capable of heating up to about 50°C, three sets of orientation Godets (with heat capability) with one additional relaxation set of Godets at the end of line prior to a collection spool. Between a second and third set of Godets, and also, between third and the final relaxation set of Godets are two annealing ovens used to bring heat into fibers to enhance its crystal formation. Depending on a particular resin studied in this report, an air cabinet capable of heating up to 60°C can be also used. This piece of equipment is usually placed between a water bath and the first set of Godets with a goal to develop enough crystallinity in a material before a drawing step. If the amount of crystallinity in a resin is too low at this point, the fiber will break or exhibit very low strength at the end of extrusion. The fiber diameter is measured online using a Mitutoyo laser Micrometer located just before a collection spool.

Extruded monofilaments were collected on spools and stored in a vacuum chamber. To ensure dimensional stability, selected PDO/Gly monofilaments were annealing at 85°C for 6 h either using the straight rack (0% relaxation) or using 5–10% rack relaxation. A rack relaxation step during annealing process may be used to lower the Young's modulus, and thus stiffness of the fiber, improving the handling characteristics.

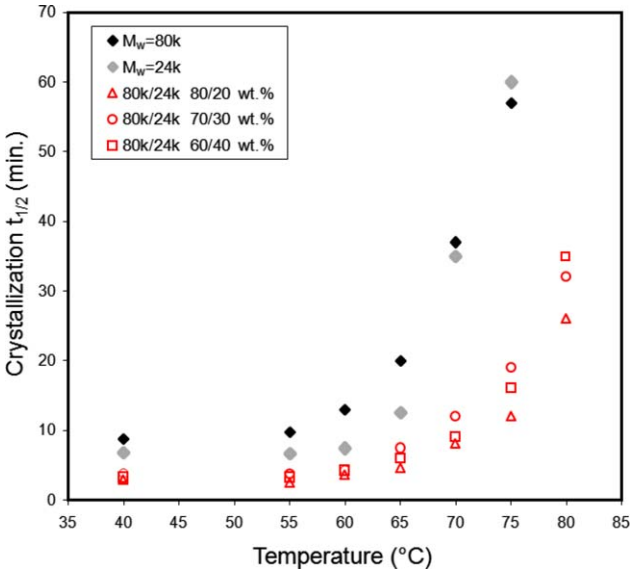

Figure 2. Isothermal crystallization kinetics of two poly(*p*-dioxanone) homopolymers (M_w = 80k and 24k) and their respective blends as measured by DSC. The figure is reprinted from the patent literature. [Color figure can be viewed in the online issue, which is available at wileyonlinelibrary.com.][51,52]

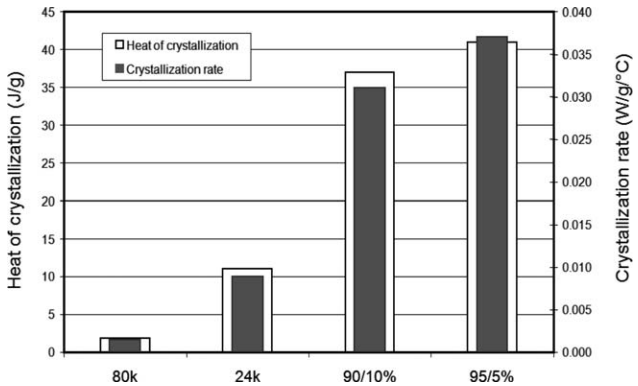

Figure 3. Nonisothermal DSC crystallization data obtained during cooling from the melt at the cooling rate of 10°C/min for PDS homopolymers having M_w = 80k and 24k, and their two bimodal, 90/10 and 95/5 (wt % 80k/wt % 24k) blends. The figure is reprinted from the patent literature.[51,52]

CASE STUDY 1—NOVEL PHYSICAL MANIPULATION METHODS: BIMODAL MOLECULAR WEIGHT EFFECT

Description of the Method

We have recently reported a novel approach to increase crystallization kinetics of polymers using what we refer to as the bimodal molecular weight effect.[55,56,91] The vast majority of experimental work was done on a variety of synthetic absorbable polyesters that are commonly used in the medical industry. In those communications we described absorbable polymer compositions that consist of physical blends of regular-to-high molecular weight polymer with a lower molecular weight counterpart of the same material as a minor component. The molecular weight of the lower molecular weight component must exceed the chain entanglement threshold, which translates to a weight-average molecular weight of approximately 10,000 Da for most polyesters.

In case of semicrystalline materials, bimodal molecular weight blends provide significantly higher crystallization rates compared with those of the individual components, resulting in enhanced processability during extrusion, melt blowing, and injection molding operations. At the same time, bimodal blends made from absorbable polymers provide more uniform and significantly faster hydrolysis rates as compared to the values obtained from the individual blend components.

We found that the presence of lower molecular weight polymer does not affect the nucleation density of the original material but greatly increases the growth rate of polymer spherulites. When compositions are produced from the blend of high and low molecular weight polymers, the overall rate of crystallization is often at least two times faster than that of either individual component.[91]

An illustration of the bimodal molecular weight effect is shown in Figures 1–3. In Figure 1, isothermal crystallization kinetics, as measured by differential scanning calorimetry (DSC), are presented for two PLLA homopolymers having weight average molecular weights of 300,000 (denoted as "300k") and 50,000 ("50k") Da and three of their respective blends. Several bimodal molecular weight PLLA blends were made (60/40, 70/30, and 80/20 wt % high M_w/wt % low M_w) by solution casting with acetone. It is worth mentioning that two PLLA homopolymers (unimodal molecular weight distribution) were prepared using the same solvent casting methods as their corresponding bimodal blends. For the DSC measurements, the samples were first melted at 200°C for 2 min and then quenched to a desired crystallization temperature to complete the crystallization process. Crystallization rates are expressed through the use of crystallization half-time values. Data in Figure 1 indicate that all bimodal blend components exhibit faster crystallization rates than the major, high molecular weight component (300k) alone at all isothermal temperatures. In the temperature range of 120°C and below, the bimodal blends show roughly identical crystallization kinetics compared with the minor, low molecular component (50k). However, at isothermal temperatures higher than 120°C, all bimodal blends show much faster crystallization than any of the individual blend components. Finally, at the high temperature range (140–150°C) the two PLLA homopolymers fail to produce any measurable indication of crystallinity as measured by the DSC, while bimodal blends still exhibit relatively fast crystallization kinetics.

A similar set of crystallization data were obtained on a different polymer system based on absorbable, dyed poly(*p*-dioxanone) (PDS) homopolymer. A variety of bimodal blends of two PDS homopolymers (80,000 and 24,000 Da) were made ranging from 60/40 to 95/5 (wt % high M_w/wt % low M_w). The blends were made via melt mixing (i.e., without the use of solvents). The two PDS homopolymers were also prepared by the same, melt mixing method as their bimodal blends. Figure 2 summarizes the DSC isothermal crystallization data conducted on individual PDS components and their bimodal blends. We found that over the range of isothermal crystallization temperature conditions explored herein, all bimodal blends (open symbols) crystallize much faster than either of the unimodal PDS components. At temperatures close to the melting point (ca., 80°C), as was the case with PLLA, individual polymer components did not produce measurable crystallization signal, though the bimodal blends crystallize rapidly.

Bimodal molecular weight blends crystallize quickly under nonisothermal conditions, as well. Figure 3 depicts the DSC crystallization kinetics data obtained during the cooling scan at 10°C/min from the melt for each of the individual PDS components as well as two of their bimodal molecular weight blends (90/10 and 95/5). The data clearly indicate that crystallization rate and heat of crystallization for both 90/10 and 95/5 bimodal blends are significantly higher than those generated by either individual component. The synergetic effect of mixed components on crystallization is particularly important for the 95/5 bimodal blend for medical applications, where high strength or toughness is required. In this particular blend composition, a presence of only 5 wt % lower molecular weight component (24,000 Da) is expected to have negligible effect on fiber's tensile properties made from this blend.

Selected Examples of Bimodal Molecular Weight Applications

Polymeric materials with fast crystallization kinetics offer great practical advantages when melt processed, especially when fabricating medical devices using an injection molding or fiber extrusion process. Rapid crystallization is particularly advantageous when injection molding articles are made from resins with low T_gs, where dimensional stability is primarily achieved through crystallization. In the absence of crystallization, injection molded parts made from polymers possessing low T_g frequently display distortion and deformation upon removal from the mold, as they are not able to withstand the forces exerted—however mild—during the removal process.

The faster that an article crystallizes, the shorter the cycle time needed. In addition to the economic benefit, short cycle times also reduce the time the polymer resides in the machine at elevated temperatures. This reduces the amount of degradation that may occur, further improving part quality. The amount of crystallinity needed in the part prior to ejection from the mold depends on the T_g of the resin as well as the molecular weight of the resin. The lower the T_g, the higher the level of crystallinity required. For the low-T_g materials reported on below, we

Table II. Calorimetric Data of Various Poly(*p*-dioxanone) Resins and Injection Molded Straps

		DSC, first heat			DSC, second heat[a]				
Sample ID	Comments	T_g (°C)	T_m (°C)	ΔH_m (J/g)	T_g (°C)	T_c (°C)	ΔH_c (J/g)	T_m (°C)	ΔH_m (J/g)
PDS-Strap	Annealed (85°C/6 h) strap from dyed PDS of $M_w = 80k$	−6	106	76	−10	**39**	47	106	56
70/30 Bimodal resin	Bimodal annealed 70/30 dyed PDS pellets	−5	107	62	−11	31	47	106	59
70/30 Bimodal Strap-Unannealed	Bimodal unannealed 70/30 dyed PDS strap	−7	108	63	−11	**29**	44	106	59
70/30 Bimodal Strap-Annealed	Bimodal annealed 70/30 dyed PDS strap	−5	108	74	−10	**30**	46	107	60
95/5 Bimodal resin	Bimodal annealed 95/5 dyed PDS pellets	−5	106	63	−10	33	33	106	53
95/5 Bimodal Strap-Unannealed	Bimodal unannealed 95/5 dyed PDS strap	−5	107	57	−10	**31**	44	106	54

[a] The samples were melted at 140°C for 2 min and then quenched (−60°C/min) to −50°C, followed by a heating scan at 10°C/min.

found that it is advantageous to have a crystallinity level of at least 10%. In the case of fibers of high molecular orientation, the level of crystallinity should be even higher, preferably more than 25%, to provide sufficient dimensional stability.

Injection Molding of Absorbable Fixation Straps. One major potential application for bimodal molecular weight technology is in injection molding processes. An example of absorbable material that can be fabricated into dimensionally stable medical devices such as fully absorbable fixation tacks (*a.k.a.*, straps) by injection molding has been recently described by our group.[92] The method uses absorbable polymer compositions in which PDS is blended with polylactide or a poly(lactide-*co*-glycolide) copolymer to produce straps with high stiffness. In this study, we instead used PDS-based resins to produce straps for medical applications where lower stiffness and faster hydrolysis time are required.

Straps were made by injection molding PDS homopolymer, as well as two bimodal molecular weight blends of PDS (70/30 and 95/5, high/low M_w). Calorimetric data of the resins and final products are summarized in Table II. The thermal transitions based on the first heat measurements are similar for all samples, suggesting similar polymer morphology. However, the second heat measurements indicate considerably faster cold crystallization rates (note the significantly lower cold crystallization temperatures, T_c) for the resins and straps made by the bimodal molecular weight method.

In Table III, injection molding conditions are listed for straps made from PDS homopolymer, as well as the two bimodal blends. Due to faster crystallization of 70/30 and 95/5 bimodal blends the total cycle time for making successful fixation straps was reduced by 60% and 40%, respectively. The significantly shorter manufacturing time would generate substantially savings, as well as limit the degree of degradation caused by prolonged exposure to high temperatures.

Fiber Extrusion—Monofilaments and Multifilaments (Braids). The use of fast crystallizing bimodal molecular weight blends is also advantageous during fiber extrusion and drawing processes, such as those used in the manufacture of surgical sutures. Materials exhibiting fast crystallization kinetics generally provide better dimensional stability with greater control of polymer morphology. Drawing of fine fibers is particularly difficult. Excessively slow crystallization will result in frequent line breaks.

We have extruded a novel, fast-crystallizing 95/5 bimodal poly(*p*-dioxanone) blend (see Table II and Figure 3) into USP size 7-0 monofilaments. We used processing conditions identical to those

Table III. Injection Molding Conditions for Manufacturing Absorbable Fixation Straps

Sample ID	Resin's melt index[a] (g/10 min)	Mold temperature (°C)	Melt temperature (°C)	Cooling time (sec)	Total cycle time (sec)
PDS-strap	0.117	28	156	72	85
70/30 bimodal strap	0.554	38	117	20	**34** (−60%)
95/5 bimodal strap	0.117	20	161	40	**51** (−40%)

[a] Melt Index measurements (MT987 Extrusion Plastometer, Tinius Olsen, Willow Grove, PA) were conducted at 150°C using 6600 g weight disc. The die diameter was 0.066 cm, while the die length was 0.800 cm.

Table IV. Tensile Properties of USP Size 7-0 Poly(*p*-dioxanone) Homopolymer of Normal Molecular Weight Distribution and 95/5 Bimodal Poly(*p*-dioxanone) Monofilaments

Fiber ID	Diameter (μm)	Straight tensile (N)	Knot tensile (N)	Elongation to break (%)	Young's modulus (kpsi)
95/5 bimodal PDS blend	88.3	5.29	4.05	36	3100
PDS of normal M_w distribution	83.8	4.09	3.60	44	2200

used to make monofilaments from poly(*p*-dioxanone) homopolymer of normal molecular weight distribution having the same size, extruder temperatures, line speed, draw ratio, and oven temperatures. The extrusion of USP size 7-0 95/5 bimodal PDS monofilament went smoothly; no line breaks were observed.

As compared to USP size 7-0 monofilament made from poly(*p*-dioxanone) homopolymer of normal molecular weight distribution, 95/5 bimodal PDS monofilament exhibits higher straight tensile and knot tensile properties, as indicated in Table IV. Elongation to break of the bimodal monofilament is lower with higher Young's Modulus, suggesting a higher molecular orientation and/or a higher level of crystallinity. Our WAXD results indicate that, a slightly higher level of crystallinity exists for the bimodal monofilament (58 vs. 55%). Evidently, a more efficient incorporation of crystals into the fiber polymer morphology occurs during extrusion which, in turn, produces a stronger monofilament.

Our next goal was to examine the postimplantation, in vivo properties for the 95/5 bimodal PDS monofilament. Specifically, the sutures need appropriate tensile strength—typically characterized by breaking strength retention (BSR)—during the required healing period. The postimplantation retention of mechanical properties is a critical feature of an absorbable medical device. The device must retain mechanical integrity until the tissue has healed sufficiently. Typically, the data used for BSR evaluations are expressed in Newtons and/or percentages. At specified time points, the tensile strength of samples was tested using an Instron mechanical property testing machine. Samples with a 2.54 cm (1 in.) gauge length were strained by the moving crosshead, programming to traverse 2.54 cm/min (1 in./min). The in vivo study was conducted in rats using USP size 7-0 monofilament made from poly(*p*-dioxanone) homopolymer of normal molecular weight distribution as the experimental control; the data are presented in Figure 4. For an additional comparison, in vivo data of two other sutures of a larger size (USP 2-0) obtained from separate experiments are also provided. Note that in vivo data has a standard error of <10%. The numbers located next to each hydrolysis curve represent total absorption (hydrolysis) times in days, determined by the in vitro automatic titration method.[94] BSR results on the 95/5 bimodal PDS monofilament indicate clearly that this fiber hydrolyzes faster and loses postimplantation tensile strength significantly faster than the PDS of normal molecular weight distribution control.

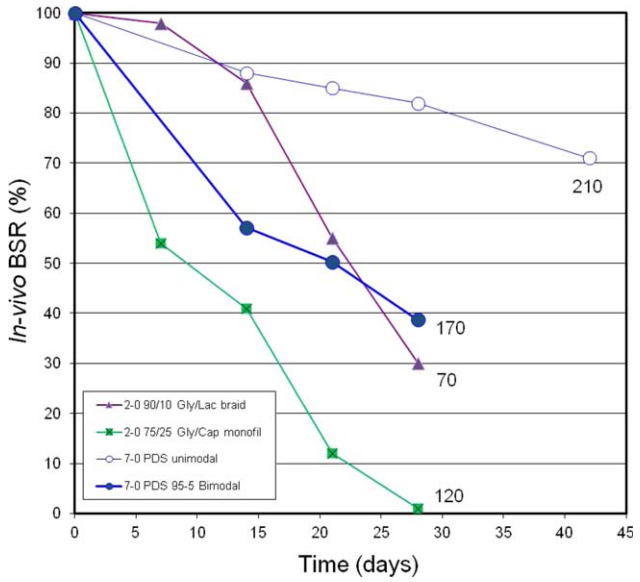

Figure 4. *In vivo* BSR of poly(*p*-dioxanone) monofilament of normal molecular weight distribution ($M_w = 80$k) and its 95/5 bimodal monofilament, also USP size 7-0. Corresponding data for two commercial sutures of the bigger size (USP 2-0) are shown also as a comparison. The numbers next to each curve represent total absorption times determined by *in vitro* automatic titration measurements. [Color figure can be viewed in the online issue, which is available at wileyonlinelibrary.com.]

The significance of this finding is that we can use the bimodal molecular weight technology to simultaneously design a medical device (e.g., sutures) with both improved mechanical properties and a shorter total absorption time. This is of particular importance for medical devices used in surgical procedures where wound healing is fast and where prolonged existence of a device may cause patient discomfort. Procedures that demand the absolute best aesthetic outcome may also benefit from the faster BSR profile, as long-lasting medical devices may, on occasion, induce unwanted foreign body reactions.

As we demonstrated with monofilament suture products, the BSR profile of long-lasting multifilament sutures can be tuned using the bimodal molecular weight approach. We produced a multifilament (braid) suture of USP size 1 composed of 95/5 poly(L(−)-lactide-*co*-glycolide) (Lac/Gly) copolymer using our bimodal molecular weight approach. The bimodal molecular weight blend is composed of 80% 95/5 Lac/Gly copolymer with a weight average molecular weight of 90,000 Da, and 20% of 95/5 Lac/Gly copolymer having a weight average molecular weight of 21,000 Da. The multifilament extrusion of this bimodal blend proceeded smoothly with a tensile strength of the annealed fiber only about 5% lower than the corresponding 95/5 Lac/Gly unimodal braid of the same size. Calorimetric data presented in Table V also revealed higher crystallinity levels in

Table V. DSC Calorimetric Properties of 95/5 Lac/Gly USP Size 1 Braids

	First heat (10°C/min)			Second heat (10°C/min)				
Braid	T_g (°C)	T_m (°C)	ΔH_m (J/g)	T_g (°C)	T_c (°C)	ΔH_c (J/g)	T_m (°C)	ΔH_m (J/g)
95/5 Lac/Gly (Unimodal)	81	170	39	57	122	32	163	32
95/5 Lac/Gly (80/20 Bimodal)	76	165	43	56	116	39	166	39

the bimodal molecular weight braid during first and second heat scans as evident from higher heat of fusion values.

The sutures were also subjected to in vitro hydrolytic degradation in a buffer at 70°C with pH maintained at 7.3. The hydrolysis data are presented in Figure 5. As an additional comparison, the hydrolysis results of a PDS monofilament of normal molecular weight distribution are also provided. It is clear that a faster crystallizing 80/20 Bimodal braid of 95/5 Lac/Gly copolymer also hydrolyzes considerably faster than the 95/5 Lac/Gly unimodal braid. Although BSR data are not available for the 95/5 Lac/Gly bimodal braid, we expect, based on the results given in Figure 5, that the loss of tensile properties post-implantation would be faster for this fiber. This would open the door to a new product opportunity: a strong, multifilament suture offering a BSR intermediate to those provided by unimodal molecular weight PDS and 95/5 Lac/Gly sutures.

Melt-Blown Nonwoven Constructs. Finally, we would like to briefly describe an important medical application of the bimodal molecular weight technology in which novel and improved melt-blown nonwoven constructs are made. Recently, we have described the melt-blown nonwoven constructs produced from absorbable poly(*p*-dioxanone) using the bimodal molecular weight approach.[93] Owing to the significantly faster crystallization rate of the bimodal polymer blend, we were able to produce nonwoven constructs with a much smaller individual filament diameter compared to those made by unimodal poly(*p*-dioxanone) homopolymer resin. A melt-blown nonwoven construct having smaller diameter size may have a profound effect on biological performance. For instance, cell-seeding may be differ on a lighter, more uniform, and flexible nonwoven substrate.[95] In addition, due to faster crystallization kinetics of the bimodal resin, we found that no release paper was necessary for collecting the construct during melt-blowing, making the manufacturing process faster, simpler, and more economical.

Proposed Mode of Action of the Bimodal Molecular Weight Effect

One hypothesis for the faster crystallization and hydrolysis rates observed in the bimodal systems is enhanced local mobility of the higher molecular weight chains. The presence of small amount of lower molecular component may serve as an "internal plasticizer" for the higher molecular weight fraction, allowing faster incorporation in the crystal lattice during spherulitic growth. Cooperative motions and enhanced diffusional capabilities would be completely lost when the molecular weight of the minor component is below chain entanglement.

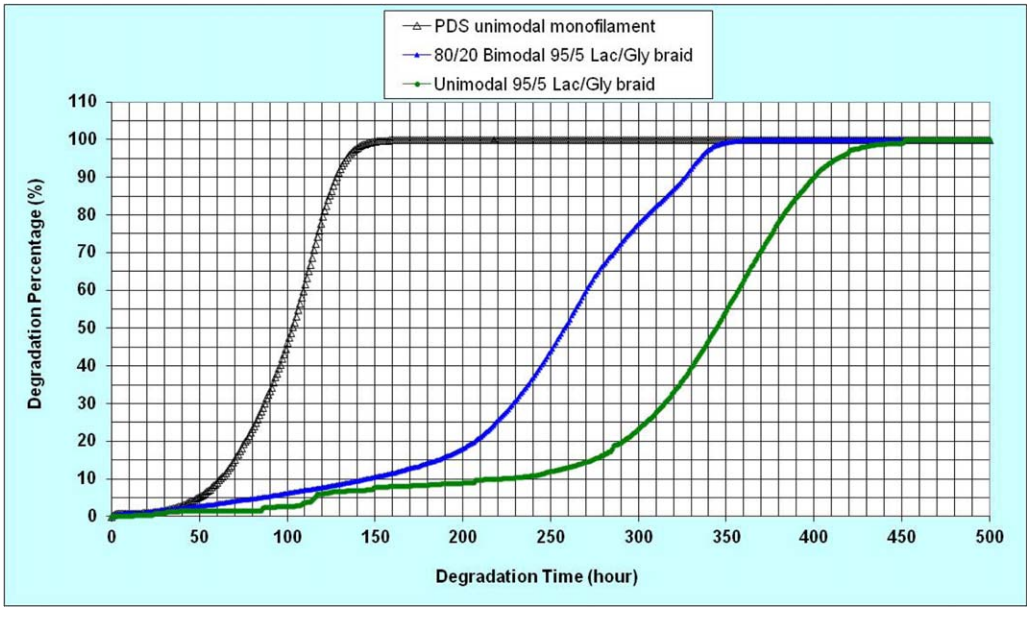

Figure 5. *In vitro* hydrolytic degradation of PDS monofilament and 95/5 Lac/Gly braid of normal molecular weight distribution, and 80/20 Bimodal 95/5 Lac/Gly braid conducted at 70°C and pH 7.3. All sutures are of USP Size 1. [Color figure can be viewed in the online issue, which is available at wileyonlinelibrary.com.]

Table VI. Synthesis of 92/8 (mol %/mol %) PDO/Gly Copolymers

Copolymer ID	DD/DEG molar ratio (%)	Monomer to initiators ratio	IV[a] (dL/g)	Mw (g/mole)
1A	100/0	~1,200 : 1	1.73	80,000
1B	75/25	~1,000 : 1	1.77	73,000
1C	50/50	~1,000 : 1	1.61	68,000
1D	25/75	~1,000 : 1	1.55	55,000
1E	0/100	~800 : 1	1.41	49,000

[a] IV was determined using HFIP at a concentration of 0.1 g/dL and a temperature of 25°C.

Therefore, oligomers would be regarded by high molecular weight component as "foreign materials" and would not engage in the cooperative motions that allow faster crystal growth. Moreover, enhanced local molecular mobility may facilitate fast diffusion of water molecules through a medical device made from bimodal molecular weight resins, causing faster hydrolysis and faster loss of tensile properties postimplantation.

CASE STUDY 2—NOVEL CHEMICAL MANIPULATION METHODS: MIXED INITIATORS APPROACH

Description of the Method

In this section we will describe the "mixed initiators" phenomenon, discovered in our laboratory about a decade ago.[96,97] If, during the course of polymerization of glycolide-containing copolymers, monofunctional and difunctional initiators are mixed and added to a reactor in a specific molar ratio, a copolymer resin is formed which exhibits significantly faster crystallization kinetics. More specifically, nucleation rate is dramatically enhanced, while the spherulitic growth rate remains practically unchanged. The important benefit of this discovery is that rapid nucleation allow for easier and more efficient extrusion and drawing of glycolide-containing copolymer systems, where crystallization kinetics are otherwise impaired.

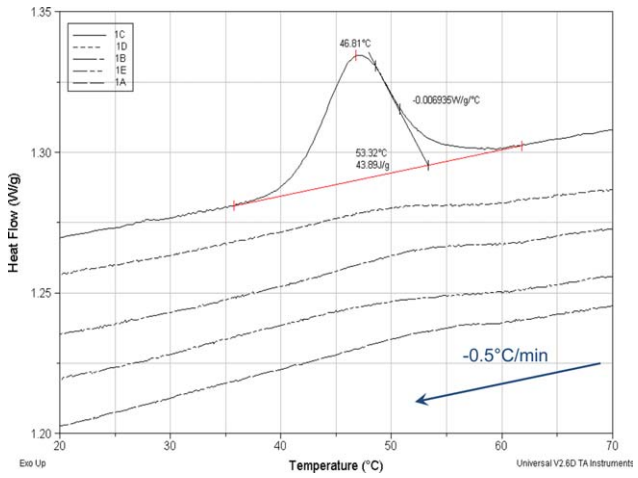

Figure 6. Nonisothermal DSC traces of studied PDS copolymers obtained during crystallization from the melt at the constant cooling rate of 0.5°C/min. Reprinted with permission from Andjelić, S.; Jamiolkowski, D. D.; Kelly, B. M.; Newman, H. *Macromolecules* 36, 8024, 2003. Copyright 2003 American Chemical Society. [Color figure can be viewed in the online issue, which is available at wileyonlinelibrary.com.]

Experimental data using the "mixed initiators" approach was generated for three glycolide-containing systems: 92/8 PDO/Gly, 75/25 poly(glycolide-co-ε-caprolactone), and 95/5 poly(L(-)-lactide-*co*-glycolide). A significant increase in the crystallization rate was observed in all cases, though the optimal ratio of mono- to difunctional initiator is different for each system.

As an illustration of this phenomenon, a series of 92/8 PDO/Gly copolymers were synthesized by ring-opening polymerization using various ratios of DD (a monofunctional initiator) to DEG (a difunctional initiator), as shown in Table VI below.

The overall crystallization rate depends heavily on two factors: the concentration of growing spherulites with time (nucleation rate) and the rate of spherulitic growth. These two processes govern the measurable output of calorimetric testing, although their individual impact is masked by their convolution. DSC data generated for samples 1A–E during cooling from the melt at a constant cooling rate (0.5°C/min) are displayed in Figure 6. The data clearly indicate extensive crystallization in copolymer 1C, made by a 50 : 50 molar ratio of monofunctional to difunctional initiators. The thermogram of copolymer 1C is characterized by a relatively large high-temperature slope and large enthalpy of crystallization as compared to other corresponding copolymers. The maximum of the crystallization peak is located at about 47°C at this constant cooling rate.

To determine which of the crystallization factors (nucleation vs. spherulitic growth) is dominant in this phenomenon, the copolymers listed in Table VI were examined under isothermal crystallization conditions (40°C for 60 min) using hot-stage optical microscopy (HSOM). The data are shown in Figure 7. As in the case of DSC measurements, extensive crystallization of copolymer 1C (50 : 50 DD : DEG ratio) was observed. A visual inspection of the crystalline morphology indicated that total crystal impingement occurred almost instantaneously, implying that the nucleation density of copolymer 1C was extremely high. Crystal growth was limited relatively early on by impingement with neighboring spherulites. Ultimately, this results in a crystalline texture composed of a large number of spherulites of very small diameter. The average diameter of the spherulites at the studied conditions (40°C after 60 min) was roughly 8 μm for copolymer 1C; the other copolymers described in Table VI had significantly higher average spherulite diameters (roughly 70 μm). The unusually strong nucleation effect for copolymer 1C was attributed to the presence of blocky glycolide sequences, which serve as effective nucleation sites and strongly facilitate subsequent crystallization of the major polymerized *p*-dioxanone component. The relatively high nucleation rate of this specific copolymer formulation is likely to produce smaller spherulites, which may be advantageous in manufacturing highly oriented absorbable sutures and small medical implantable devices.

In the next section we will present novel data on the effective use of this technology in manufacturing medical implantable devices based on poly(*p*-dioxanone) and glycolide copolymers.

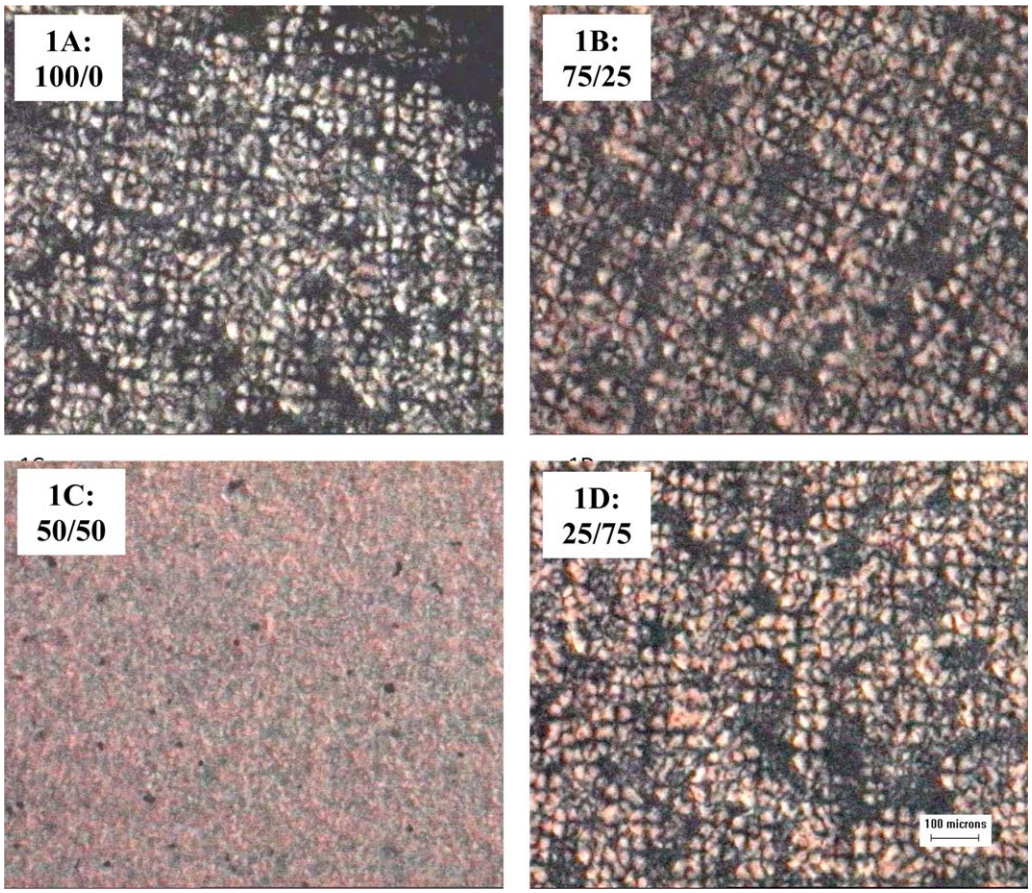

Figure 7. HSOM images of copolymers 1A–D examined under isothermal crystallization conditions (40°C for 60 min). The numbers shown in the images represent DD/DEG ratios used to synthesize these copolymers. Reprinted with permission from Andjelić, S.; Jamiolkowski, D. D.; Kelly, B. M.; Newman, H. *Macromolecules* 36, 8024, 2003. Copyright 2003 American Chemical Society. [Color figure can be viewed in the online issue, which is available at wileyonlinelibrary.com.]

Application of the Mixed Initiators Method for Novel Medical Devices

Unmet Need in Polymer Processing industry. The mixed initiator copolymers described here either crystallize at a faster rate and/or to a higher extent as compared with their copolymers made with either monofunctional initiator or difunctional initiator alone. Crystallizing at a higher rate has advantages when melt processing the copolymers made by this method. This is especially true when fabricating medical devices using a technique such as injection molding or fiber extrusion processes.

In injection molding processes, polymers that crystallize rapidly allow for crystallization of the part while still in the mold (as opposed to after ejection). Here the mold cavity not only acts to define the shape of the part but also act to restrain the shape of the part during the crystallization process. With more difficult-to-crystallize polymers, the part needs to be ejected from the mold before complete polymer morphology development takes place, the cycle time becomes prohibitively long to prevent part deformation, and the injection molding process becomes impractical. Rapid crystallization is particularly advantageous during fabrication of articles from resins with low T_gs,

Table VII. Tensile Properties of Selected Drawn and Annealed 2-0 PDO/Gly Monofilaments Made by Mixed Initiators

Sample ID	Description	Diameter (μm)	Tensile strength (N)	Tensile strength (MPa)	Elongation (%)	Knot (N)	Young's modulus (MPa)
Fiber 1–6.25x draw	Annealed at 85°C for 6 h with 0% rack relaxation	366	50.3	476	39	27	1,520
Fiber 2–7.50x draw	Annealed at 85°C for 6 h with 5% rack relaxation	368	64.1	600	51	30	1,000
Fiber 3–8.50x draw	Annealed at 85°C for 6 h with 5% rack relaxation	361	73.4	717	41	34	1,240

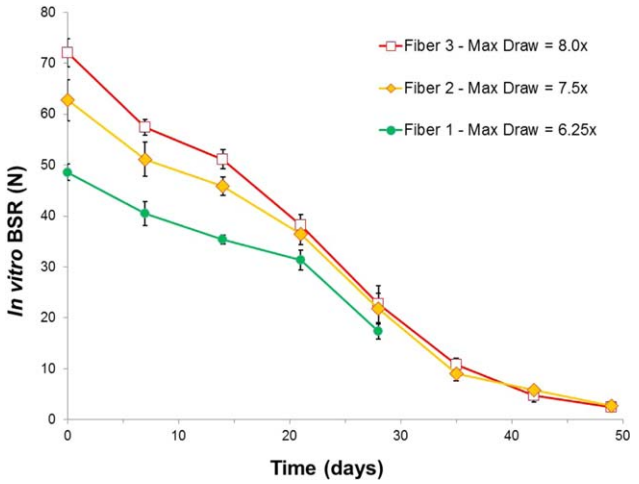

Figure 8. *In vitro* BSR properties (in Newtons) of the selected 2-0 drawn and annealed 92/8 PDO/Gly monofilaments made from mixed initiators but with the different molecular orientation. [Color figure can be viewed in the online issue, which is available at wileyonlinelibrary.com.]

because dimensional stability is primarily achieved through polymer crystallization for this class of materials. The amount of crystallinity needed in the part prior to ejection from the mold depends on the T_g of the resin, as well as the molecular weight of the resin. In general, the lower the T_g, the higher the level of crystallinity required.

In the case of fiber extrusion processes, low fiber crystallinity prior to drawing results in the inability to apply a load effectively. The fiber will not draw or crystallize further but will instead sag on the fiber line, or even break. Moreover, the fiber can shrink significantly during downstream processing, thereby losing molecular orientation and, consequently, its tensile strength. In many cases, crystallization rate is a critical parameter; optimization of this characteristic may lead to a successful product or to failure—no fiber at all.

Physical Properties of 92/8 Block PDO/Gly Copolymers made by Mixed Initiators Method. As expected, during monofilament extrusion, a 92/8 PDO/Gly copolymer made by a single initiator only (Example 1 in Table I) failed to produce the high fiber properties despite using a wide range of processing conditions, including the use of an air cabinet to achieve higher level of crystallinity. The fiber sagged on the line and broke frequently before being able to draw it to higher molecular orientation. The explanation put forward is that the copolymer resin of Example 1 nucleated and crystallized too slowly during the processing, preventing the fiber from "locking in" the needed polymer morphology and maintaining its molecular orientation at a higher level.

On the other hand, 92/8 PDO/Gly copolymers made by the 50 : 50 DD : DEG mixed initiators (Examples 2 and 3 in Table I) produced strong fibers. Selected tensile properties of fibers made by this method are displayed in Table VII below.

We observed that too much crystallinity may also produce certain undesirable processing challenges. For instance, the sample named "Fiber 1-6.25x draw" in Table VII, was made from 92/8 PDO/Gly resin of inherent viscosity, IV = 1.85 dL/g. During the extrusion process of this material, a smaller air gap of 1.9 cm (0.75 in.) was used along with an air cabinet leading to only a maximum achievable draw ratio of 6.25×. Operating at a lower draw ratio is a direct consequence of excessive crystallinity prior to the first drawing step. In addition, the fiber was annealed using the same conditions as other fibers in Table VII but with 0% rack relaxation; this contributed to higher fiber stiffness (Young's Modulus). To achieve higher draw ratios in extruded monofilaments, we took full advantage of rapid nucleation of these resins and purposely limited the amount of crystallinity in an extrudate before the first drawing step. This was done by removing an air cabinet unit from the extrusion line and increasing the air gap (distance between a die and a surface of water) to allow for more chain relaxation of a melt extrudate. The resulting fibers (samples named Fiber 2-7.50x draw and Fiber 3-8.50x draw in Table VII) show outstanding physical properties including very high tensile strength. In addition, a rack relaxation step during annealing procedure reduced stiffness that aided in better handling characteristics.

Absorbable sutures made by fibers exemplified in Table VII are designed to have the requisite physical characteristics to assure desirable BSR profile. In some bodily tissues, healing occurs more slowly, requiring an extended retention of mechanical integrity. This is often associated with tissue that has poor vascularization.[98,99] Likewise, there are other situations in which a given patient may be prone to poor healing, for example, the diabetic patient. In vitro BSR measurements on fibers listed in Table VII were conducted at physiologically relevant in vitro conditions: 7.27 pH buffer solution maintained at 37°C temperature. In addition to in vitro measurements, we also obtained in vivo BSR data on "Fiber 2-7.50x draw" monofilament. The data indicated excellent agreement between *in vitro* and *in vivo* data for this copolymer system. BSR for the rest of the samples was obtained using the *in vitro* method only.

As an illustration of improved processing steps of the resins made by this new process, BSR properties of the selected 2-0 drawn and annealed 92/8 PDO/Gly monofilaments made from mixed initiators but with different molecular orientation are shown in Figure 8. Data in Figure 8 strongly suggest higher initial tensile strength values and longer BSR profiles for samples drawn to higher extent.

We also found that 92/8 PDO/Gly copolymers made by mixed initiators used in the novel absorbable monofilament sutures undergo no significant morphological changes (degradation, transesterification, and so on) during various steps of thermal processing. This includes the ability of material to crystallize rapidly. As we discussed earlier, rapid crystallization is important to provide a robust and reliable manufacturing process to enable the very high strength exhibited by these fibers, as well as allowing for effective retention of mechanical strength as a function of time postimplantation.

Summary

In the first case study, we described a novel, powerful method of increasing the crystallization rate of a given polymer system

without introducing new chemical species or using various means of melt shear enhancement. Bimodal molecular weight blends described here are composed of regular molecular weight polymer as a major component and a minor component of the same polymer having lower molecular weight (albeit above the chain entanglement threshold for the polymer of interest). Bimodal molecular weight blends show significantly faster crystallization kinetics (due primarily to a relatively high spherulitic growth) than either of the individual components alone. This synergetic effect is quite strong and allows for making various medical devices with unique mechanical and biological properties, including sutures, meshes, films, microspheres, nonwoven constructs, and injection molding parts. Bimodal molecular weight blends, if made from absorbable components, exhibit faster hydrolysis rates than those of the individual blend components. This modification in performance opens new possibilities for medical devices where faster hydrolysis rates are needed, including, for instance, drug delivery applications.

In the second case study, we showed that novel absorbable sutures and fibers made by mixed monofunctional and difunctional initiators have numerous advantages. Due to very high nucleation rates detected in these copolymers, new and improved melt processing procedures were used, resulting in favorable product performance. For instance:

- Suture with high tensile strength but lower Young's modulus can be made;
- BSR profiles suitable for mid-term surgical applications are possible;
- Excellent knot sliding and knot security behavior can be achieved;
- Good pliability/handling properties.

Additional fiber advantages include the capability of being "barbed" by conventional cutting and forming processes, and the capability of being processed into other conventional medical devices, including but not limited to surgical fabrics, such as meshes.

ACKNOWLEDGMENTS

The authors wish to thank Benjamin D. Fitz and Brian M. Kelly—both of Ethicon, Inc.—for their valuable help in executing these studies. Additionally, we thank Dennis D. Jamiolkowski for his guidance and helpful feedback.

REFERENCES

1. Yeh, G. S. Y. *Polym. Eng. Sci.* **1976**, *16*, 138.
2. Yeh, G. S. Y. *Polym. Eng. Sci.* **1976**, *16*, 145.
3. Yeh, G. S. Y.; Hong, K. Z. *Polym. Eng. Sci.* **1979**, *19*, 395.
4. Haas, T. W.; Maxwell, B. *Polym. Eng. Sci.* **1969**, *9*, 225.
5. Kobayashi, K.; Nagasawa, T. *J. Macromol. Sci., Part B: Phys.* **1970**, *4*, 331.
6. Lagasse, R. R.; Maxwell, B. *Polym. Eng. Sci.* **1976**, *16*, 189.
7. Wolkowicz, M. D. *J. Polym. Sci.: Polym. Symp.* **1978**, *63*, 365.
8. Sherwood, C. H.; Price, F. P.; Stein, R. S. *J. Polym. Sci.: Polym. Symp.* **1978**, *63*, 77.
9. Ulrich, R. D.; Price, F. P. *J. Appl. Polym. Sci.* **1976**, *20*, 1077.
10. Abuzaina, F. M.; Fitz, B. D.; Andjelić, S.; Jamiolkowski, D. D. *Polymer* **2002**, *43*, 4699.
11. Somani, R. H.; Hsiao, B. S.; Nogales, A.; Fruitwala, H.; Srinivas, S.; Tsou, A. H. *Macromolecules* **2001**, *34*, 5902.
12. Zhong, Y.; Fang, H.; Zhang, Y.; Wang, Z.; Yang, J.; Wang, Z. *ACS Sustain. Chem. Eng.* **2013**, *1*, 663.
13. Kumaraswamy, G.; Issaian, A. M.; Kornfield, J. A. *Macromolecules* **1999**, *32*, 7537.
14. Kumaraswamy, G.; Kornfield, J. A.; Yeh, F.; Hsiao, B. S. *Macromolecules* **2002**, *35*, 1762.
15. Tang, H.; Chen, J.-B.; Wang, Y.; Xu, J.-Z.; Hsiao, B. S.; Zhong, G.-J.; Li, Z.-M. *Biomacromolecules* **2012**, *13*, 3858.
16. Samon, J. M.; Schultz, J. M.; Hsiao, B. S. *Polymer* **2002**, *43*, 1873.
17. McHugh, A. J. *J. Appl. Polym. Sci.* **1975**, *19*, 125.
18. Mackley, M. R.; Keller, A. *Philos. Trans. Roy. Soc. Lond. Series A, Math. Phys. Sci.* **1975**, *278*, 29.
19. Rao, I. J.; Rajagopal, K. R. *Int. J. Solids Struct.* **2001**, *38*, 1149.
20. Stein, R. S. *Polym. Eng. Sci.* **1976**, *16*, 152.
21. Stein, R. S.; Rhodes, M. B. *J. Appl. Phys.* **1960**, *31*, 1873.
22. Yau, W.; Stein, R. S. *J. Polym. Sci. Part B: Polym. Lett.* **1964**, *2*, 231.
23. Yau, W.; Stein, R. S. *J. Polym. Sci. Part A-2: Polym. Phys.* **1968**, *6*, 1.
24. Kumaraswamy, G.; Verma, R. K.; Kornfield, J. A.; Yeh, F.; Hsiao, B. S. *Macromolecules* **2004**, *37*, 9005.
25. Kukalyekar, N.; Balzano, L.; Peters, G.; Rastogi, S.; Chadwick, J. *Macromol. React. Eng.* **2009**, *3*, 448.
26. Kimata, S.; Sakuri, T.; Nozue, Y.; Kasahara, T.; Yamaguchi, N.; Karino, T.; Shibayama, M.; Kornfield, J. A. *Science* **2007**, *316*, 1014.
27. Fernandez-Ballester, L.; Thurman, D. W.; Zhou, W.; Kornfield, J. A. *Macromolecules* **2012**, *45*, 6557.
28. Seki, M.; Thurman, D. W.; Obchrhauser, J. P.; Kornfield, J. A. *Macromolecules* **2002**, *35*, 2583.
29. Chen, Y.-H.; Mao, Y.-M.; Li, Z.-M.; Hsaio, B. S. *Macromolecules* **2010**, *43*, 6760.
30. Bin, H.; Gale, D. C. US Pat. 2007.
31. Rubinstein, M.; Colby, R. H. Polymer Physics; Oxford university Press: Oxford, **2003**.
32. Toki, S.; Che, J.; Rong, L.; Hsiao, B. S.; Amnuaypornsri, S.; Nimpaiboon, A.; Sakdapipanich, J. *Macromolecules* **2013**, *46*, 5238.
33. Toki, S.; Hsiao, B. S.; Amnuaypornsri, S.; Sakdapipanich, J. *Polymer* **2009**, *50*, 2142.
34. Pan, P.; Liang, Z.; Zhu, B.; Dong, T.; Inoue, Y. *Macromolecules* **2008**, *41*, 8011.
35. Loo, Y. L.; Wakabayashi, K.; Huang, E.; Register, R. A.; Hsiao, B. S. *Polymer* **2005**, *46*, 5118.

36. Alizadeh, A.; Richardson, L.; Xu, J.; McCartney, S.; Marand, H.; Cheung, Y. W.; Chum, S. *Macromolecules* **1999**, *32*, 6221.
37. Marx, C. L.; Cooper, S. L. *J. Macromol. Sci., Part B: Phys.* **1974**, *9*, 19.
38. Wakabayashi, K.; Register, R. A. *Macromolecules* **2006**, *39*, 1079.
39. Scogna, R. C.; Register, R. A. *Polymer* **2008**, *49*, 992.
40. Scogna, R. C.; Register, R. A. *Polymer* **2009**, *50*, 585.
41. Sear, R. P. *Nat. Mater.* **2011**, *10*, 809.
42. Ponting, M.; Lin, Y.; Keum, J. K.; Hiltner, A.; Baer, E. *Macromolecules* **2010**, *43*, 8619.
43. Andjelić, S.; Jamiolkowski, D. D.; McDivitt, J.; Fischer, J.; Zhou, J. J. *J. Polym. Sci.: Part B: Polym. Phys.* **2001**, *39*, 3073.
44. Chen, S.; Zhang, Y.; Fang, H.; Ding, Y.; Wang, Z. *CrystEngComm* **2013**, *15*, 5464.
45. Kit, K. M. *Polymer* **1988**, *39*, 4969.
46. Napolitano, S.; Wübbenhorst, M. *Macromolecules* **2006**, *39*, 5967.
47. Martínez-Tong, D. E.; Vanroy, B.; Wübbenhorst, M.; Nogales, A.; Napolitano, S. *Macromolecules* **2014**, *47*, 2354.
48. Vanroy, B.; Wübbenhorst, M.; Napolitano, S. *ACS Macro Lett.* **2013**, *2*, 168.
49. Fitz, B. D.; Jamiolkowski, D. D.; Andjelić, S. *Macromolecules* **2002**, *35*, 5869.
50. Jin, J.; Du, J.; Chen, H.; Han, C. C. *Polymer* **2011**, *52*, 6161.
51. Jin, J.; Chen, H.; Muthukumar, M.; Han, C. C. *Polymer* **2013**, *54*, 4010.
52. Pan, P.; Shan, G.; Bao, Y. *Ind. Eng. Chem. Res.* **2014**, *53*, 3148.
53. Arai, F.; Takeshita, H.; Dobashi, M.; Takenaka, K.; Miya, M.; Shiomi, T. *Polymer* **2012**, *53*, 851.
54. Loo, Y. L.; Register, R. A. *Macromolecules* **2001**, *34*, 8968.
55. Andjelić, S.; Fitz, B. D. Ethicon, Inc. US Pat. 8,450,431, 2013.
56. Andjelić, S.; Fitz, B. D. Eur. Pat. 1979412 B1, **2009**.
57. Carvalho, J. L.; Cormier, S. L.; Lin, N.; Dalnoki-Veress, K. *Macromolecules* **2012**, *45*, 1688.
58. Elmoumni, A.; Gonzalez-Ruiz, R. A.; Coughlin, E. B.; Winter, H. H. *Macromol. Chem. Phys.* **2005**, *206*, 125.
59. Mercier, J. P. *Polym. Eng. Sci.* **1990**, *30*, 270.
60. Rybnikar, F. *J. Appl. Polym. Sci.* **1969**, *13*, 827.
61. Schiraldi, D. A. In Modern Polyesters; Sheirs, J., Long, T. E., Eds.; John Wiley & Sons Ltd.: West Sussex, England, **2003**, Chapter 6.
62. Pan, P.; Liang, Z.; Cao, A.; Inoue, Y. *ACS Appl. Mater. Interf.* **2009**, *1*, 402.
63. Li, L.; Hood, M. A.; Li, C. Y. *Polymer* **2009**, *50*, 953.
64. Beck, H. N. *J. Appl. Polym. Sci.* **1967**, *11*, 673.
65. Beck, H. N.; Ledbetter, H. D. *J. Appl. Polym. Sci.* **1965**, *9*, 2131.
66. Binsbergen, F. L. *Polymer* **1970**, *11*, 253.
67. Liu, C.-K. United States Surgical Corporation, US Pat. 5,997,568, **1999**.
68. Pan, P.; Yang, J.; Shan, G.; Bao, Y.; Weng, Z.; Inoue, Y. *Macromol. Mater. Eng.* **2012**, *297*, 670.
69. Qiu, Z.; Li, Z. *Ind. Eng. Chem. Res.* **2011**, *50*, 12299.
70. Tsui, A.; Frank, C. W. *Polymer* **2014**, *55*, 6364.
71. Pan, P.; Liang, Z.; Nakamura, N.; Miyagawa, T.; Inoue, Y. *Macromol. Biosci.* **2009**, *9*, 585.
72. López-Rubio, A.; Gavara, R.; Lagarón, J. M. *J. Appl. Polym. Sci.* **2006**, *102*, 1516.
73. Porter, M. M.; Yu, J. *J. Biomater. Nanobiotechnol.* **2011**, *2*, 301.
74. Makarewicz, P. J.; Wilkes, G. L. *J. Polym. Sci.: Polym. Phys. Ed.* **1978**, *16*, 1529.
75. Durning, C. J.; Rebenfeld, L.; Russel, W. B. *Polym. Eng. Sci.* **1986**, *26*, 1066.
76. Crank, J. The Mathematics of Diffusion; Oxford University Press: Oxford, **1975**.
77. Desai, A. B.; Wilkes, G. L. *J. Polym. Sci.: Symp.* **1974**, *46*, 291.
78. Sheldon, R. P.; Blakey, P. R. *Nature* **1962**, *195*, 172.
79. Baker, W. O.; Fuller, C. S.; Pape, N. R. *J. Am. Chem. Soc.* **1942**, *64*, 776.
80. Spence, J. *J. Phys. Chem.* **1941**, *45*, 401.
81. Zhai, W.; Yu, J.; Ma, W.; He, J. *Polym. Eng. Sci.* **2007**, *47*, 1338.
82. Yu, L.; Liu, H.; Dean, K.; Chen, L. *J. Polym. Sci.: Part B: Polym. Phys.* **2008**, *46*, 2630.
83. Napolitano, S.; Wübbenhorst, M. *Macromolecules* **2006**, *39*, 5967.
84. van Bennekom, A. C. M.; Gaymans, R. *J. Polymer* **1997**, *38*, 657.
85. Andjelić, S.; Richard, R. S. *Macromolecules* **2001**, *34*, 896.
86. Dikovsky, D.; Marom, G.; Avila-Orta, C. A.; Somani, R. H.; Hsiao, B. S. *Polymer* **2005**, *46*, 3096.
87. Jamiolkowski, D. D.; Dormier, E. In An Introduction to Biomaterials; Hollinger, J. O., Ed.; CRC Press, Taylor & Francis Group: Boca Raton, FL, **2012**, Chapter 15.
88. Murdock, J. R.; Loomis, G. L. US Pat. 4,719,246 and 4,766,182, **1988**.
89. Loomis, G. L.; Murdock, J. R.; Gardner, K. *Transactions of the 15th Annual Meeting of Society of Biomaterials* **1989**, *12*, 73.
90. Schmidt, S. C.; Hillmyer, M. A. *J. Polym. Sci. Part B: Polym. Phys.* **2001**, *39*, 300.
91. Andjelić, S.; Fitz, B. D. *PMSE Preprints 95*, 821, **2006**.
92. Kelly, B. M.; Jamiolkowski, D. D.; DeFelice, C. US Pat. 2012/0071566, **2012**.
93. Andjelić, S.; Fitz, B. D.; Zhou, J. J. US Pat. 8,236,904, **2012**.
94. Fitz, B. D.; Jamiolkowski, D. D. *J. Biomed. Mater. Res. B: Appl. Biomater.* **2013**, *101B*, 1014.
95. Ajji, A.; Moreno, M.; Bureau, M. US Pat. 8,318,618 B22012.

96. Andjelić, S.; Jamiolkowski, D. D.; Kelly, B. M.; Newman, H. *Macromolecules* **2003**, *36*, 8024.

97. Newman, H.; Andjelić, S.; Kelly, B. M.; Jamiolkowski, D. D.; Bezwada, R. US Pat. 6,794,484 and 6,831,149, **2004**.

98. Gross, G. H. *Pathobiology* **2013**, *80*, 203.

99. Letic-Gavrilovic, A.; Bakos, D. In Polymeric Materials; Caruta, B., Ed.; Nova Science Publishers, Inc.: Hauppauge, NY, **2005**.